Surface Damage Induced by FIB Milling and Imaging of Biological Samples is Controllable

DAMJANA DROBNE,[1]* MARZIALE MILANI,[2] VLADKA LEŠER,[1] AND FRANCESCO TATTI[3]
[1]*Department of Biology, University of Ljubljana, SI-1000 Ljubljana, Slovenia*
[2]*Materials Science Department and Laboratory FIB/SEM "Bombay," University of Milano-Bicocca, I-20125 Milano, Italy*
[3]*FEI Italia, I-20122 Milano (MI), Italy*

KEY WORDS FIB/SEM; FIB damage; conductive staining; terrestrial isopod; digestive glands; electron microscopy

ABSTRACT Focused ion beam (FIB) techniques are among the most important tools for the nanostructuring of surfaces. We used the FIB/SEM (scanning electron microscope) for milling and imaging of digestive gland cells. The aim of our study was to document the interactions of FIB with the surface of the biological sample during FIB investigation, to identify the classes of artifacts, and to test procedures that could induce the quality of FIB milled sections by reducing the artifacts. The digestive gland cells were prepared for conventional SEM. During FIB/SEM operation we induced and enhanced artifacts. The results show that FIB operation on biological tissue affected the area of the sample where ion beam was rastering. We describe the FIB-induced surface major artifacts as a melting-like effect, sweating-like effect, morphological deformations, and gallium (Ga^+) implantation. The FIB induced surface artifacts caused by incident Ga^+ ions were reduced by the application of a protective platinum strip on the surface exposed to the beam and by a suitable selection of operation protocol. We recommend the same sample preparation methods, FIB protocol for milling and imaging to be used also for other biological samples. *Microsc. Res. Tech. 70:895–903, 2007.*

INTRODUCTION

Focused ion beam (FIB) techniques are among the most important tools for the nanostructuring of surfaces and microstructure characterization (Li, 2006). The FIB is widely used in semiconductor industry and material sciences, and most recently it has entered into life sciences (Ballerini et al., 1997; Drobne et al., 2004, 2005a,b; Ishitani et al., 1995; Milani et al., 2006a,b).

FIB instruments were used for eroding biological material and exposing subsurface structures as early as in 1960's (Claugher, 1986; Fulker et al., 1973; Lewis et al., 1968; Spector et al., 1974). However, the difficulties with interpretation of the results and uncertainty about the side effects of ion manipulation have placed serious limitations on the broad application of ion etching in biology. In spite of this, the results indicated that ions and fast atom sources can reveal the biological structures in a way that cannot be achieved by any other method (Haggis, 1982; Ishitani et al., 1995; Li et al., 2001; Yonehara et al., 1989).

Recently, the FIB/SEM system proved the applicability for site-specific exposing of subsurface structures of biological samples prepared either for conventional scanning electron microscopy (Drobne et al., 2004, 2005a,b), and of unprepared cells (Milani and Drobne, 2006). A challenge of the present time remains to differentiate the true structure from artifacts and to control them and to assess the potential of FIB/SEM in life sciences.

In a FIB machine, the samples are irradiated with positively charged Ga ions produced by a liquid metal ion source (LMIS) and usually accelerated to the energy of 30–50 keV. The beam profile has a shape consisting of a core with the Gaussian type of current-density distribution. Typical beam diameters may be as low as 5–7 nm. In addition to this core, the focused ion beam shows long-range tails with a current density typically three–four orders of magnitude lower than the maximum current density and decays approximately with distance from the beam center (Frey et al., 2003).

FIB nanostructuring involves rastering a beam of ions across a sample. The momentum of the ions as they strike the sample surface is so high that some material, atoms and ions, is sputtered away (Frey et al., 2003; Haswell et al., 2003). FIB is governed by different parameters given by the beam profile, by the angle of incidence, by ion species, ion dose, ion energy, etc. During FIB milling, the interaction of highly energetic (30 keV) gallium ion beam with the sample surface has many not desirous side effects. The FIB induced artifacts are described as morphological defects, crystal damage, uncontrolled Ga^+ implantation, amorphization, material redeposition, mixing of material, radiation damage, changes in surface geometry, and its electronic properties, etc. (Adams, 2006; Barber, 1993; Barna et al., 1999; Bever et al., 1992;

*Correspondence to: Damjana Drobne, Department of Biology, University of Ljubljana, Večna pot 111, SI-1000 Ljubljana, Slovenia.
E-mail: damjana.drobne@bf.uni-lj.si

Received 30 May 2006; accepted in revised form 15 March 2007

Contract grant sponsor: Ministry of Education, Science and Sport of the Government of the Republic of Slovenia; Contract grant number: J1-3186; Contract grant sponsor: Italian Ministry for Foreign Affairs and the Slovenian Ministry of Education, Science and Sport; Contract grant number: BI-IT/05-08-022.

DOI 10.1002/jemt.20494

Published online 27 July 2007 in Wiley InterScience (www.interscience.wiley.com).

Boxleitner et al., 2001; Brezna et al., 2003; Cairney and Munroe, 2003; Frey et al., 2003; Huang, 2004; Inkson et al., 2006; Ishitani et al., 1998, 2004; McCaffrey et al., 2001; Nord et al., 2002; Perrey et al., 2004; Rajsiri et al., 2002; Reiner et al., 2004; Rubanov and Munroe, 2003, 2004, 2005; Stanishevsky et al., 2002; Vetterli et al., 1995; Wang et al., 2005; Yabuuchi et al., 2004; Yu et al., 2006).

All these artifacts have two characteristics even in materials that are made by few elements and have simple 2D geometries: they are not easily predictable in detail (quantitatively) and they are strongly interconnected, i.e., they are simultaneously developing and mutually influencing.

The depth and width of the damaged subsurface volume is very difficult to assess (Vetterli et al., 1995). It has been found that both, the effective sputter rate and the damage depth, increase with increasing beam energy (Boxleitner et al., 2001). Also, the low intensity tail regions give rise to extended gallium contamination. Moreover, beam tail regions with lower ion fluency than core regions face different effects than the center part of the structures. The thickness of the damaged layers is greater than that calculated from theoretical models of ion implantation (Rubanov and Munroe, 2005). These differences are explained by the dynamic nature of FIB milling, meaning that the energetic ion beams pass through already damaged layers.

During milling operation, the surface damage caused by incident ions can be reduced by metallic (Adams et al., 2006; Arnold and Bauer, 2003; Haswell et al., 2003; Rubanow and Munroe, 2003; Reiner et al., 2004) or carbon (Thompson et al., 2006) barrier layers covering the specimen. After milling, the damaged layer can be reduced by final mills at low accelerating voltages (few kV), by plasma cleaning, and by polishing, also known as "clean-up cuts," etc. (Cairney and Munroe, 2003; Kato, 2004; Rubanov and Munroe, 2003; Wang et al., 2005). In final polishing, the beam is rastered line by line towards the region of interest and can significantly reduce the artifacts because of redeposition, amorphisation, and morphological defects known as curtaining (Cairney et al., 2000 a,b).

Beyond the effects associated with FIB sectioning, also FIB imaging can modify the target and the exposed sections. Actually a consequence of FIB imaging (scanning ion microscopy, SIM) is also the progressive destruction of the imaged surface. Here, the destructive nature of SIM can be used as a tool for a gradual removal of the exposed layers thus uncovering the structures beneath (Ohya and Ishitani, 2003a,b; Sakai et al., 1999). At SIM, the FIB-sample interaction is not taken as an artifact that is needed to be reduced, but to be controlled.

In biological samples, there is a lack of information about deformations induced by FIB milling or imaging. The low ion beam current polishing (typically 100 to 300 pA) can be used to reduce the damaged layer (Drobne et al., 2004, 2005a,b; Ishitani et al., 1995). Otherwise, not much is known about the surface damage induced by FIB.

The aim of our study was to document the consequences of FIB interactions with biological sample surface during FIB milling and imaging operation, identify the classes of artifacts, and test procedures that could induce quality of (FIB milled) sections by reducing the artifacts. The single layer epithelium of isopod crustacean digestive glands was prepared for scanning electron microscopy. The investigated sample surface was gold sputtered. In places, a platinum strip was deposited for protection of the surface from the ion beam. Secondary ion (SI), secondary electron (SE), and backscattered electron (BSE) imaging were performed on differently prepared tissue. We discuss the appearance, reduction, and control of FIB-sample interaction artifacts.

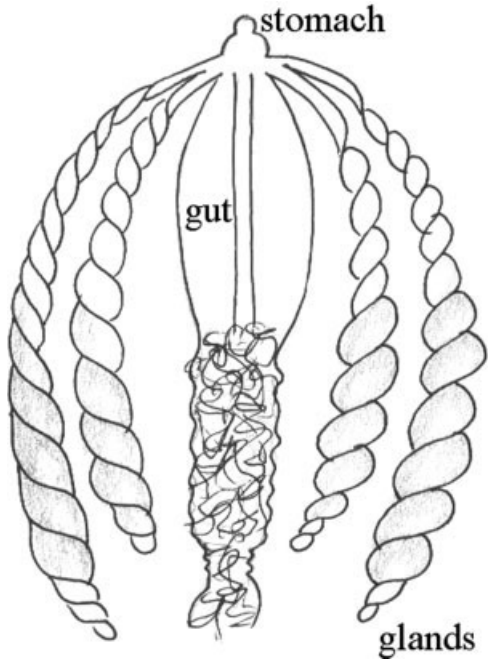

Fig. 1. Digestive system of *P. scaber* is composed of stomach, gut, and four blind ending digestive gland tubes (hepatopancreas).

MATERIALS AND METHODS

Terrestrial isopods, *Porcellio scaber* (Isopoda, Crustacea), were collected under concrete blocks and pieces of decaying wood (Ljubljana, Slovenia).

Digestive system of a terrestrial isopod *Porcellio scaber* is composed of a gut, a stomach, and four blind ending digestive gland tubes, which are up to 8 mm long and can reach 0.5 mm in diameter (Fig. 1). Digestive glands (hepatopancreas) consist of a single layer epithelium, whose cells are covered by microvilli and face the gland lumen.

After a manual break of one digestive gland tube, the apical part of gland cells became exposed for FIB/SEM investigation (Fig. 2).

Digestive gland tubes were isolated and fixed in 1.0% glutaraldehyde and 0.4% paraformaldehyde in 0.1 M sodium cacodylate buffer (pH 7.2) for 2.5 h at room temperature. The chemically fixed samples were followed by OTOTO conductively staining (OsO_4/thiocarbohydrazide/OsO_4/thiocarbohydrazide/OsO_4) (Dunnebier et al., 1995) and dehydration, or chemically fixed samples were directly dehydrated. The conductive staining introduced metals into the sample in

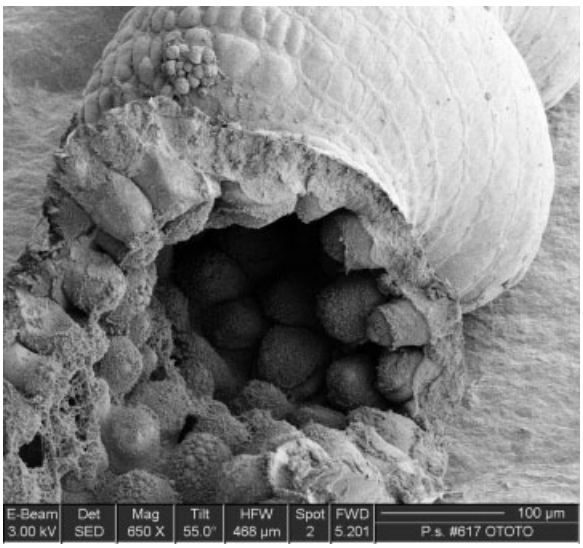

Fig. 2. Secondary electron micrograph of a manually broken digestive gland tube exposing the gland lumen. Apical parts of epithelial cells that are facing the gland tube lumen are covered by microvoli.

order to increase its conductivity. After dehydration in a graded series of ethanol, the samples were dried at the critical point (Balzers Critical Point Dryer 030) and gold coated (Sputter coater SCD 050, BAL-TEC, Germany). Digestive glands of altogether eight animals were investigated by the FIB/SEM system.

The samples were fixed on brass holders with silver paint (High purity silver paint, SPI), mounted on the sample holder into the specimen chamber (5-axis eucentric stage) of a Dual Beam system for FIB/SEM operation (FEI Strata DB 235 M). The rough milling conditions to open a trench employed ion currents of 5–7 nA, at 30 kV. Lower beam currents of 100–300 pA were used to polish the cross section. Spot size in the case of rough milling was $\sim$150–100 nm of diameter and for polishing it ranged from 20 to 35 nm of diameter. Secondary electron detectors were: Everhardt Thornely Detector (ETD), Continuous Dynode Electron Multiplier (CDEM), and Back-Scattered Electron, secondary ion detector was a CDEM. Dwell time for milling was 1 µs and the overlap was 50%. The SEM imaging was performed by means of the FEG electron column available in the same system with a resolution of 1 nm at 30 kV. The spot size in the case of SEM was up to 0.5 nm in diameter. The system operated with column pressures in the 10^{-5} Pa range and the specimen chamber pressure between 10^{-4} and 10^{-3} Pa.

RESULTS

Digestive system of a terrestrial isopod *Porcellio scaber* is composed of a gut, a stomach, and four blind ending digestive gland tubes, which are up to 8 mm long and can reach 0.5 mm in diameter (Fig. 1). Digestive glands (hepatopancreas) consist of a single layer epithelium, whose cells are covered by microvilli and face the gland lumen (Figs. 2–4). After a manual break of one digestive gland tube, the apical parts of cells became exposed for FIB/SEM investigation (Fig. 2). When a biological sample is prepared for SEM following standard preparation protocol it is usually gold or carbon coated. In our study the samples were gold sputtered.

A low ion beam current (1 nA down to 300 pA) was used for cutting a spherical structure lying on the top of microvilli (Figs. 3a and 3b). This spherical structure is most probably extruded by a neighboring cell during the extrusion phase of the cell cycle. After this operation, a melting-like effect was observed in and around the area exposed to the incident ion beam (Fig. 3b). After five successive low ion current scans of the same surface region one can observe morphological distortions of the microvilli and the most apical part of the cell lying just beneath the microvilli (Fig. 3c).

A high ion beam current (5–7 nA) was used for milling a cell in order to expose intracellular structures (Figs. 4–6). The top (apical) cell surface with microvilli was oriented against the ion beam. The milling operation was in the direction from the apical part of the cell toward its basal region. The high ion beam current milling operation produced severe morphological anomalies on the apical part of the cell and on the milled side wall and just beneath the top surface (Figs. 4a and 4b). These anomalies were successfully reduced by applying a protective platinum (Pt) strip on the apical cell surface just before milling (Figs. 4c and 4d). Here, the Pt strip protected the surface from high ion beam currents during milling as well as it creates a homogenous and nearly flat surface where the ions impact, thus reducing drastically the sputter rate difference because of the surface morphology.

The FIB exposed cell interior of a conductively stained cell was imaged by secondary (Figs. 5a–5c) and backscattered electrons (Fig. 5d) as well as by ions (Fig. 6e). A high magnification of a FIB milled cell interior reveal a high quality cut (Fig. 5a). After FIB imaging, structural defects on the imaged surface appeared that are described as morphological distortions (Figs. 5b, 6f) and bright spots (Figs. 5b and 5c). The bright appearance of these spots in secondary electron images and in backscattered electron images suggests the presence of a relatively high atomic number material (Fig. 5d). They appear only on osmium conductively stained samples. We classify their appearance as a consequence of a sweating-like effect. Most probably these spots are generated by combination of Os and Ga, as it happens also with other metals (Au, Cu, GaAs compound), where the very same effect is observed.

In samples without any conductive staining, whose cell interior was exposed by a manual break, a poor electrical conductivity lead to a charging effect at secondary electron as well as at backscattered electron imaging (Figs. 6a and 6b). After FIB milling, the charging effect was reduced and a better signal was achieved at both SE and BSE imaging (Figs. 6c and 6d). No structural deformations or changes in compositional contrast due to Ga^+ implantation were observed.

Further, this region was ion imaged (Fig. 6e). Destructive ion imaging caused rounded edges and enlarged holes. Also, ion imaging significantly improved the signal at subsequent electron imaging. We explain this improvement in the BSE and SE signal as a result of Ga^+ implantation. Ion imaging also concurs in this improvement, since it neutralizes the charge during the subsequent electron beam imaging, resulting in

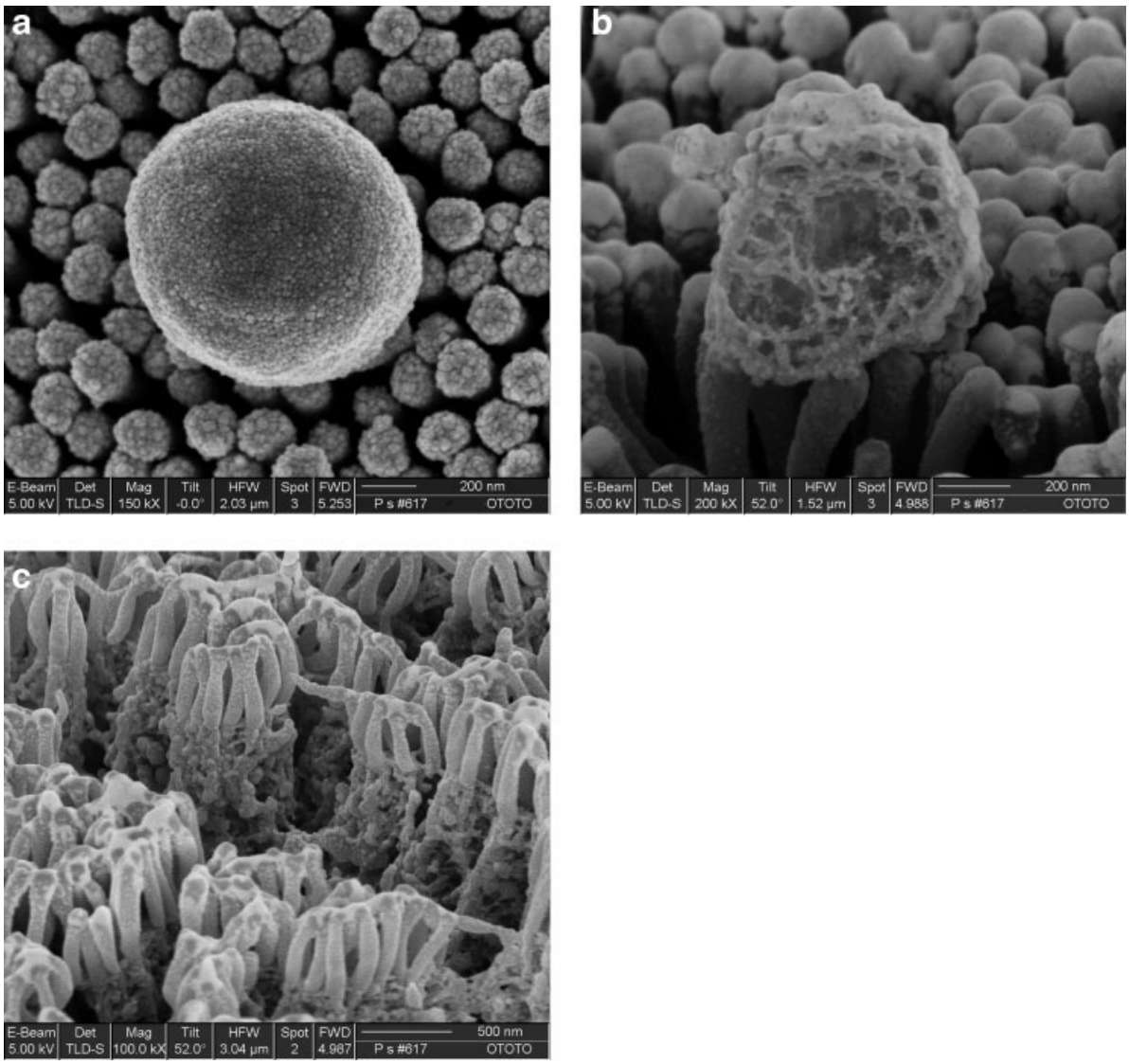

Fig. 3. **a–c:** Secondary electron micrographs of the apical cell surface before (a) and after (b, c) FIB operation. Sometimes, on the top of microvilli sphaerical structures are situated. Low ion current FIB was used for milling of one spherical structure (b); note the melting-like effect on the top of the milled structure and around the milled area (b). After successive low ion current scans of the same region, morphological distortions of the surface appear (c).

higher signal/noise ratio (Fig. 6e). No bright spots were observed after ion irradiation of exposed cell surfaces of nonconductively stained samples. The melting-like effect appears as a homogenous bright cover over the ion irradiated (scanned) gold coated surface. The two preparation methods differ significantly in the amount of Os introduced into the sample during sample preparation. In our investigation, the melting-like effect was observed only where significant amounts of metals were added either by gold sputtering on the sample surface or intracellular by postfixation and conductive staining.

DISCUSSION

FIB milling and imaging of biological tissue affect the upper sample surface exposed against the incident ion beam as well as affects side-walls during milling operation. We describe the FIB induced artifacts as a melting-like effect, a sweating-like effect, as morphological deformations, and as Ga^+ implantation.

In any case, a lot of significant images and useful information can be acquired by these FIB sustained procedures. First of all the quality of the cut can be appreciated and the possibility of selecting polygonal (and not simply linear) sectioning profiles is worth while being mentioned.

The FIB—Sample Interaction Effects

In our samples, the damaged layer induced by ion beam irradiation on gold coated surfaces of both, conductively stained or unstained samples, is described as a melting-like effect.

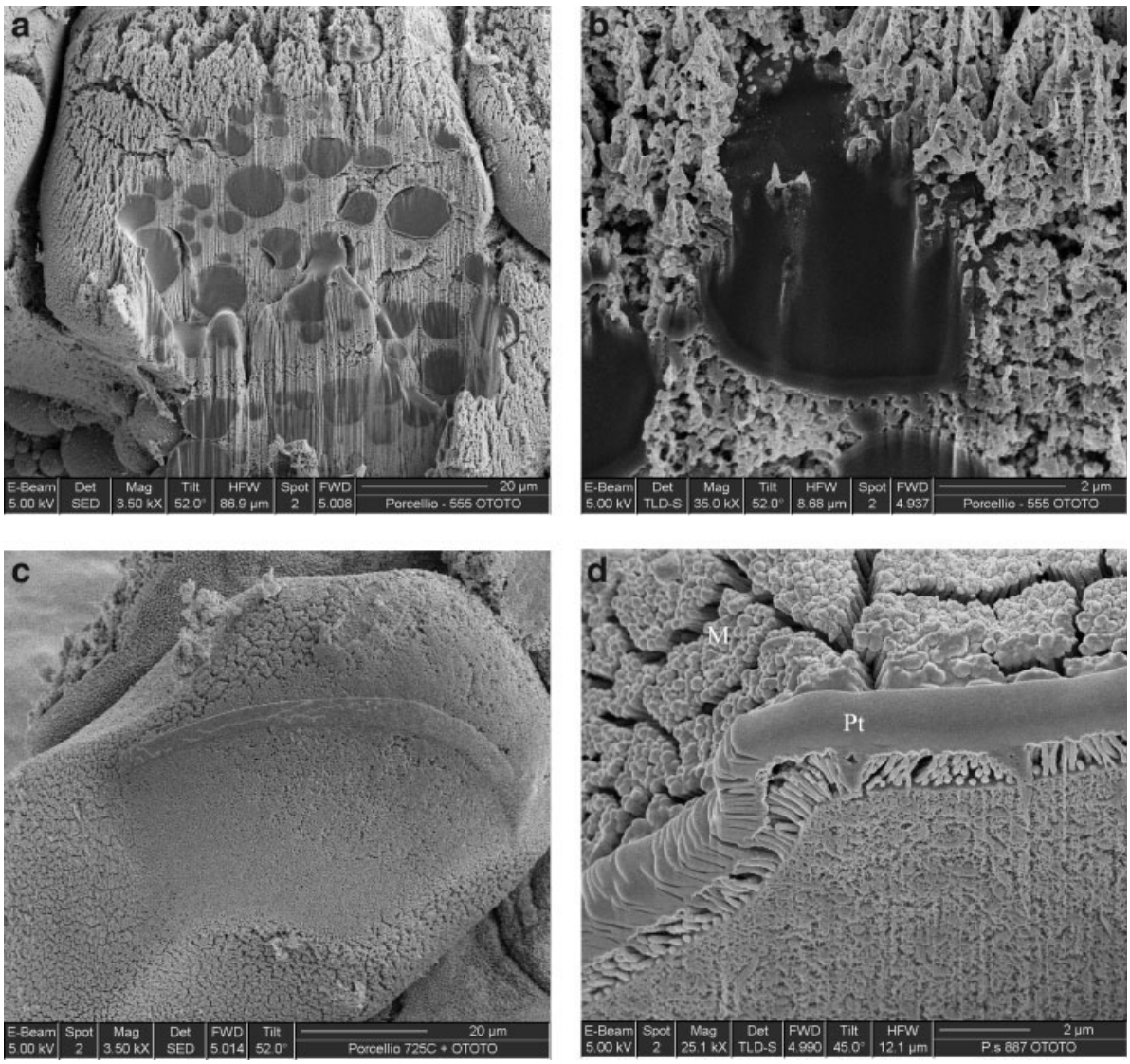

Fig. 4. **a**–**d**: Secondary electron micrographs of high ion current FIB milled cell (a, b) and of high ion current FIB milled Pt protected cell (c – before FIB milling, d – after FIB miling). Note the differences in the integritiy of the exposed intracellular regions (b, c). In (c) Pt, platinum strip; M, microvilli.

As far as bright spots are concerned, Reiner et al. (2004) report Ga^+ droplets as a result of FIB manipulation and explain their formation as a result of material redeposition. Also, there could be a reaction between the gold coating and the Ga ion beam to form Au-Ga phases and various Au-Ga intermetallics. A similar effect has been well documented on FIB milling Cu where Cu-Ga phases were identified (Phaneuf et al., 2003). In our samples the bright spots were found also on those cellular regions that appeared homogenous (lipid droplets) before ion imaging. This indicates either redeposition of the sputtered material or metal redistribution due to the local heating of the poor thermal conductive sample during FIB manipulation. No bright spots were observed in non-conductively stained FIB exposed and FIB imaged surfaces. Such samples are considered as "metal poor" samples. Therefore the sweated-like pattern caused by Ga^+ ion irradiation seems to be related to sample composition (metal content).

The most evident effects of FIB are morphological deformations. Repetitive FIB scans with low (from 1 nA down to 300 pA) ion currents resulted in material removal on the exposed layer and lead to morphological deformation of the surface and subsurface structures. The material removal correlates with the number of successive FIB scan operations. At FIB milling, differences in sputtering rates at different points produce a curtain-like effect on the milled side-walls. These are easy to recognize and more evident at the bottom of a milled trench/surface.

Another well studied FIB induced artifact is the implantation of Ga^+ ions (Cairney et al., 2000b; Ishitani et al., 1998; Reiner et al., 2004; Rubanov and Munroe,

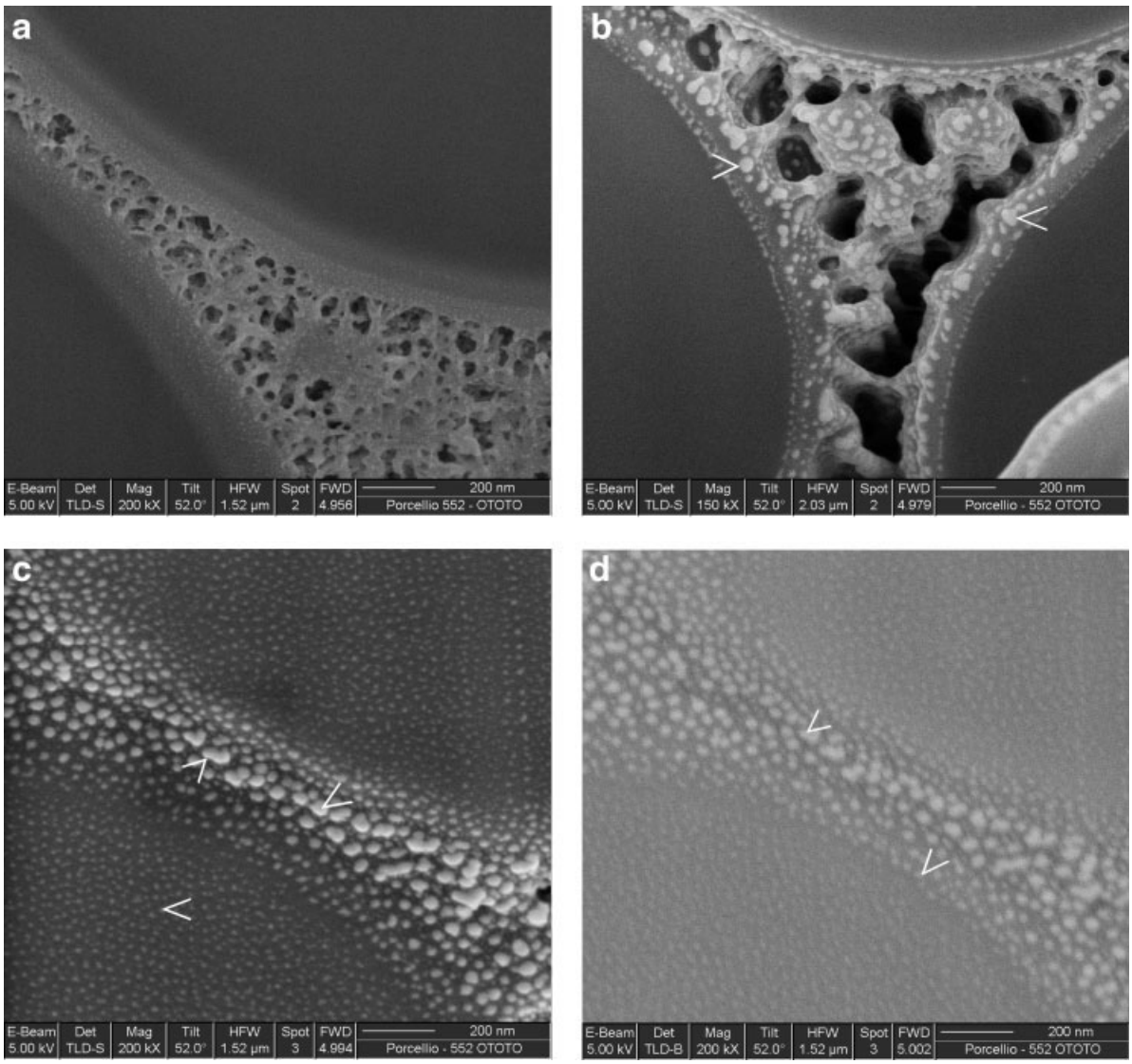

Fig. 5. **a**–**d**: Secondary electron micrographs of FIB exposed cell interior of conductively stained cells before (a) and after (b, c) FIB irradiation (scanning). Backscattered electron micrograph of FIB irradiated cell interior (d). <, bright spot-like deposits.

2003; Yu et al., 2006). To observe the FIB induced Ga^+ implants, backscattered electron (BSE) imaging of manually broken and FIB milled surfaces were compared. It was expected that the significant Ga^+ implant is recognized by different contrast on BSE images when FIB manipulated and non-manipulated surfaces are compared, since the intensity of the BSE signal is mainly a function of the average atomic number of the local area of the sample; therefore those parts of the sample which contain metals are highlighted in contrast to the unstained background (Scrivener, 2004). We found out that FIB manipulated and nonmanipulated samples did not differ in contrast pattern when imaged by BSE. However, we found significant differences in the intensity of BSE and SE signal that was much better in FIB manipulated samples. We confirm the results of other authors, that a small amount of Ga^+ is implanted on the side-wall of a trench during the milling process. They report both, the uniform or nonuniform Ga^+ implantation pattern (Haswell et al., 2003; Reiner et al., 2004).

Strategies to Minimize the Damage of FIB—Sample Interaction

Our experimental results and those published in the literature suggest that the side wall damage can be largely reduced by using low ion current polishing mill termed also "clean-up cut" (Cairney and Munroe, 2003; Chaiwan et al., 2002; Ishitani et al., 2004; Rubanov and Munroe, 2004). Milling at low currents can remove the layer of damage left by high-energy ions. The reduction of sidewall damage can be achieved also by low-kV FIB polishing at the final step (Barna et al., 1999; Boxleitner et al., 2001; Ishitani et al., 2004; Kato,

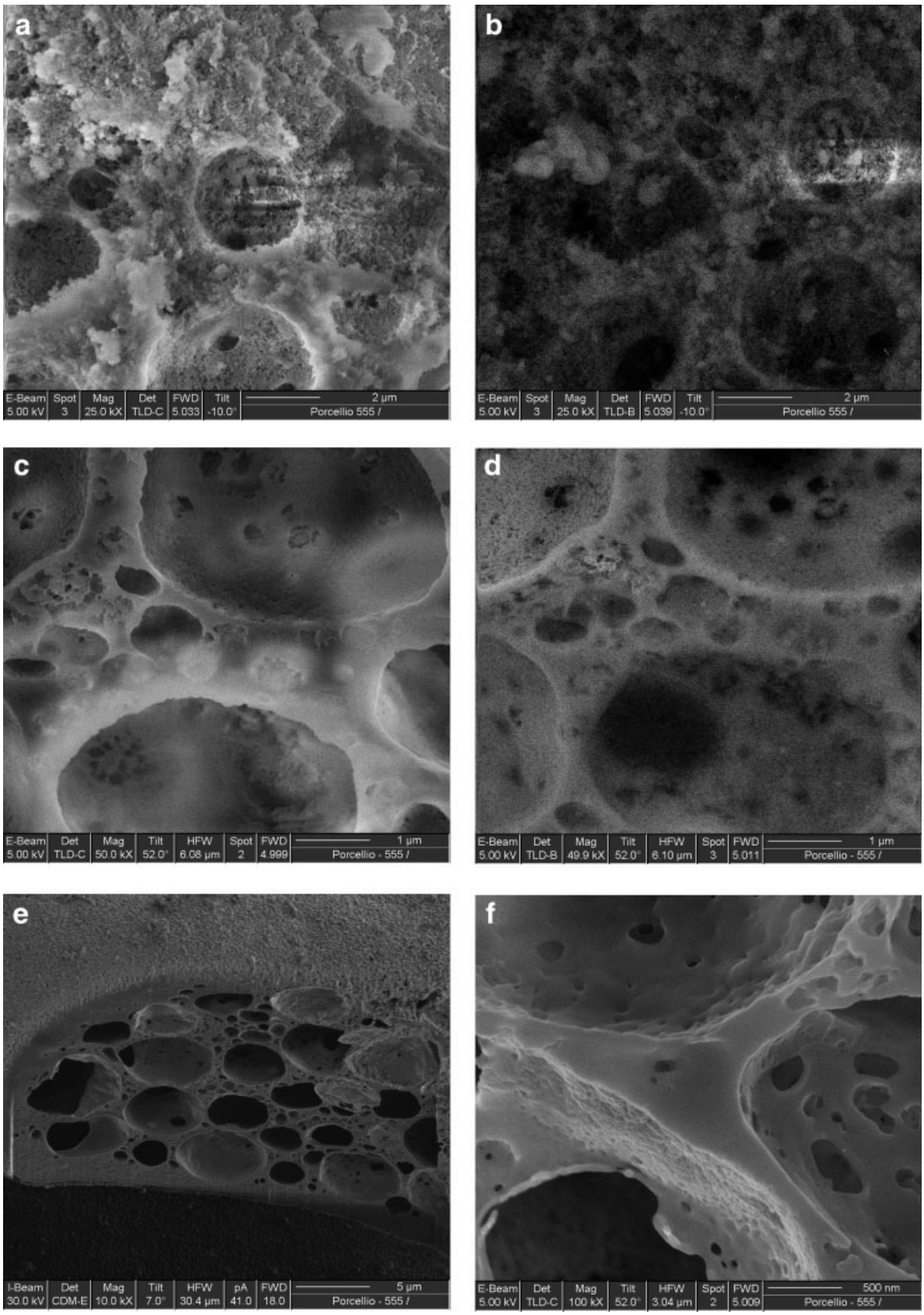

Fig. 6. **a–f:** Secondary electron micrograph of cell interior of lipid extracted cells exposed by a manual break (a). Backscattered electron micrograph of lipid extracted cells exposed by a manual break (b). Secondary electron micrograph of cell interior of lipid extracted cells exposed by FIB milling (c). Backscattered electron micrograph of lipid extracted cells exposed by FIB milling (d). Secondary electron micrograph of cell interior of lipid extracted cells after successive FIB scans (e). Scanning ion micrograph of FIB exposed cell interior (f).

2004; Lipp et al., 1995; Nebiker et al., 1997; Wang et al., 2005).

The sample surface exposed against the incident ion beam was reported to be successfully protected by metal (Adams et al., 2006; Arnold and Bauer, 2003; Reiner et al., 2004; Rubanow and Munroe, 2003) or carbon (Thompson et al., 2006) film deposited prior to FIB operation. Our results show that the gold sputtered film sufficed when small structures ($\sim$1 μm) or shallow trenches ($\sim$4 μm deep, results not shown) are milled with low beam currents; when a larger cell portion is milled, a 1–2 μm thick platinum strip was deposited on the top of the area of interest to sufficiently protect the upper sample surface from damage during the FIB operations.

CONCLUSIONS

The development of TEM and SEM started at the same time, but TEM reached its full potential for biological imaging almost 30 years earlier than SEM (Pawley, 1997). An important reason for this delay may be that the early SEMs accustomed the users to operate with a much higher beam voltage than it was necessary to produce low-resolution images of biological samples, thus stimulating the search for other techniques. These were in many cases less suitable than the optimized SEM for biological samples. Likewise, the SEM users believe that scanning electron microscopes are not suited for subsurface investigations and they switch from using SEM to TEM, from one sample to another from one scale to another, which may result in losing important information. Perhaps also here, the upgraded SEM that allows in situ controlled and precise sample manipulation is probably the optimal choice for many imaging needs in biology.

The FIB milling or imaging of digestive gland cells damage the upper sample surface exposed against the incident ion beam and the side-walls of the milled trenches. The major artifacts are described as a melting-like effect, morphological deformations or Ga^+ implantation.

a. The melting like effect appears as a homogenous bright cover over the ion irradiated (scanned) gold coated surface or on FIB milled side-walls. We explain the melting-like effect as a result of the target exposure to a high dose of ions that "*strongly*" modify the surface.
b. Morphological deformations were observed on surfaces exposed against the incident ion beam after FIB imaging or FIB milling.
c. Ga^+ implantation was detected indirectly by the reduced charging effect and improved signal at BSE and SE imaging. No structural deformations or changes in compositional contrast due to Ga^+ implantation were observed.
d. Sample preparation affected the FIB induced sweating-like effect. Bright spots were not observed after FIB imaging of subsurface structures of not post-fixed and not conductively stained samples.
e. The damage caused by incident Ga^+ ions was reduced by the gold sputtered layer or by application of protective Pt strip. The FIB milling artifacts on the side-walls were reduced by low current cleaning mill.
f. The knowledge of the nature of induced artifacts and the procedures to control and minimize them enable us to produce high reliable morphological information by FIB/SEM operations. Proof of that are the high resolution images of ultrastructural elements of cells, when major artifact control procedures are applied.
g. Serial sectioning procedures, even along orthogonal planes, and controlled etching of thin foil of materials from the milled section are possible and help in 3D imaging of structures at scales of the order of 20 nm.

In conclusion, we believe that the same sample preparation method, FIB procedures and sample surface protection can be extended to other samples, cells or tissues of biological and medical interest.

ACKNOWLEDGMENTS

We thank Ben Lich from FEI Company for stimulating the discussion about the interaction between FIB and a biological sample.

REFERENCES

Adams DP, Mayer TM, Vasile MJ, Archuleta K. 2006. Effects of evolving surface morphology on yield during focused ion beam milling of carbon. Appl Surf Sci 252:2432–2444.

Arnold B, Bauer HD. 2003. Experiences in cross section preparation of layered materials by FIB-method. Prakt Metallogr-Pr M 40:109–129.

Ballerini M, Milani M, Costato M, Squadrini F, Turcu ICE. 1997. Life science applications of focused ion beams (FIB). Eur J Histochem 4:89–90.

Barber DJ. 1993. Radiation-damage in ion-milled specimens—Characteristics, effects and methods of damage limitation. Ultramicroscopy 52:101–125.

Barna A, Pécz B, Menyhard M. 1999. TEM sample preparation by ion milling/amorphization. Micron 30:267–276.

Bever T, Jager-Waldau G, Eckberg M, Heyen ET, Lage H, Wieck AD, Ploog K. 1992. Lateral spreading of focused ion-beam-induced damage. J Appl Phys 72:1858–1863.

Boxleitner W, Hobler G, Klüppel V, Cerva H. 2001. Simulation of topography evolution and damage formation during TEM sample preparation using focused ion beams. Nucl Instrum Methods B 175/177:102–107.

Brezna W, Wanzenböck H, Lugstein A, Bertagnolli E, Gornik E, Smoliner J. 2003. Scanning capacitance microscopy investigations of focused ion beam damage in silicon. Physica E 19:178–182.

Cairney JM, Munroe PR. 2003. Redeposition effects in transmission electron microscope specimens of FeAl-WC composites prepared using a focused ion beam. Micron 34:97–107.

Cairney JM, Munroe PR, Schneibel JH. 2000a. Examination of fracture surfaces using focused ion beam milling. Scripta Mater 42:473–478.

Cairney JM, Smith RD, Munroe PR. 2000b. Transmission electron microscope specimen preparation of metal matrix composites using the focused ion beam miller. Microsc Microanal 6:452–462.

Chaiwan S, Hoffman M, Munroe P, Stiefel U. 2002. Investigation of sub-surface damage during sliding wear of alumina using focused ion-beam milling. Wear 252:531–539.

Claugher D. 1986. A summary of ion beam etching of biological material with special reference to the saddle field source. Scan Electron Microsc I:139–149.

Drobne D, Milani M, Ballerini M, Zrimec A, Berden Zrimec M, Tatti F, Drašlar K. 2004. Focused ion beam for microscopy and *in situ* sample preparation: application on a crustacean digestive system. J Biomed Opt 9:1238–1243.

Drobne D, Milani M, Zrimec A, Berden Zrimec M, Tatti F, Drašlar K. 2005a. Focused ion beam/scanning electron microscopy studies of *Porcellio scaber* (Isopoda, Crustacea) digestive gland epithelium cells. Scanning 27:30–34.

Drobne D, Milani M, Zrimec A, Lešer V, Berden Zrimec M. 2005b. Electron and ion imaging of gland cells using the FIB/SEM system. J Microsc 219:29–35.

Dunnebier EA, Segenhout JM, Kalicharan D, Jongebloed WL, Wit HP, Albers FWJ. 1995. Low-voltage field-emission scanning electron microscopy of non-coated guinea-pig hair cell stereocilia. Hearing Res 90:139–148.
Frey L, Lehrer C, Ryssel H. 2003. Nanoscale effects in focused ion beam processing. Appl Phys A 76:1017–1023.
Fulker MJ, Holland L, Hurley RE. 1973. Ion etching of organic materials. Scan Electron Microsc III:379–386.
Haggis GH. 1982. Contribution of scanning electron microscopy to viewing internal cell structure. Scan Electron Microsc II:151–163.
Haswell R, McComb DW, Smith W. 2003. Preparation of site-specific cross-sections of heterogeneous catalysts prepared by focused ion beam milling. J Microsc 211:161–166.
Huang Z. 2004. Combining Ar ion milling with FIB lift-out techniques to prepare high quality site-specific TEM samples. J Microsc 215:219–223.
Inkson BJ, Leclere D, Elfallagh F, Derby B. 2006. The effect of focused ion beam machining on residual stress and crack morphologies in alumina. J Phys: Conference Series 26:219–222.
Ishitani T, Hirose H, Tsuboi H. 1995. Focused-ion-beam digging of biological specimens. J Electron Microsc 44:110–114.
Ishitani T, Koike H, Yaguchi T, Kamino T. 1998. Implanted gallium ion concentrations of focused-ion-beam prepared cross sections. J Vac Sci Technol B 16:1907–1913.
Ishitani T, Umemura K, Ohnishi T, Yaguchi T, Kamino T. 2004. Improvements in performance of focused ion beam cross-sectioning: aspects of ion-sample interaction. J Electron Microsc 53:443–449.
Kato NI. 2004. Reducing focused ion beam damage to transmission electron microscopy samples. J Electron Microsc 53:451–458.
Lewis SM, Osborn JS, Stuart PR. 1968. Demonstration of an internal structure within the red blood cell by ion etching and scanning electron microscopy. Nature 220:614–616.
Li J. 2006. The focused-ion-beam microscope—More than a precision ion milling machine. JOM 58:27–31.
Li J, Stein D, McMullan C, Branton D, Aziz MJ, Golovchenko JA. 2001. Ion-beam sculpting at nanometre length scales. Nature 412:166–169.
Lipp S, Frey L, Franz G, Demm E, Petersen S, Ryssel H. 1995. Local material removal by focused ion beam milling and etching. Nucl Instrum Methods B 106:630–635.
McCaffrey JP, Phaneuf MW, Madsen LD. 2001. Surface damage formation during ion-beam thinning of samples for transmission electron microscopy. Ultramicroscopy 87:97–104.
Milani M, Drobne D. 2006. Focused ion beam manipulation and ultramicroscopy of unprepared cells. Scanning 28:148–154.
Milani M, Simone S, Tatti F. 2006a. FIB/SEM for soft matter and life sciences. GIT Imag Microsc 3:38–40.
Milani M, Drobne D, Drobne S, Tatti F. 2006b. An atlas of FBI/SEM applications in soft materials and life sciences, (A05, 16). Aracne, Italy: Roma.
Nebiker PW, Döbeli M, Mühle R, Suter M. 1997. Minimizing radiation damage in silicon structured with low energy focused ion beams. Nucl Instrum Methods B 127-128:897–900.
Nord J, Nordlund K, Keinonen J. 2002. Amorphization mechanism and defect structures in ion-beam-amorphized Si, Ge, and GaAs. Phys Rev B 65:165329.
Pawley J. 1997. The development of field-emission scanning electron microscopy for imaging biological surfaces. Scanning 19:324–336.
Perrey CR, Carter CB, Michael JR, Kotula PG, Stach EA, Radmilovic VR. 2004. Using the FIB to characterize nanoparticle materials. J Microsc 214:222–236.
Phaneuf M, Li J, Shuman RF, Noll K, Casy JD. 2003. Apparatus and method for reducing differential sputter rates. US Pat no. 6, 641,705. Available at www.freepatentsonline.com/6641705.html
Ohya K, Ishitani T. 2003a. Comparative study of depth and lateral distributions of electron excitation between scanning ion and scanning electron microscopes. J Electron Microsc 52:291–298.
Ohya K, and Ishitani T. 2003b. Simulation study of secondary electron images in scanning ion microscopy. Nucl Instrum Methods B 202:305–311.
Rajsiri S, Kempshall B, Schwarz S, Giannuzzi L. 2002. FIB damage in silicon: Amorphization or redeposition? Microsc Microanal 8: 50–51.
Reiner JC, Nellen P, Sennhauser U. 2004. Gallium artefacts on FIB-milled silicon samples. Microelectron Reliab 44:1583–1588.
Rubanov S, Munroe PR. 2003. The effect of the gold sputter-coated films in minimising damage in FIB-produced TEM specimens. Mater Lett 57:2238–2241.
Rubanov S, Munroe PR. 2004. FIB-induced damage in silicon. J Microsc 214:213–221.
Rubanov S, Munroe PR. 2005. Damage in III-V compounds during focused ion beam milling. Microsc Microanal 11:446–455.
Sakai Y, Yamada T, Suzuki T, Ichinokawa T. 1999. Contrast mechanisms of secondary electron images in scanning electron and ion microscopy. Appl Surf Sci 145:96–100.
Scrivener KL. 2004. Backscattered electron imaging of cementitious microstructures: Understanding and quantification. Cement Concrete Comp 26:935–945.
Spector M, Burns LC, Kimzey SL. 1974. Ion beam etching of red blood cells and latex spheres. Nature 247:61–62.
Stanishevsky A, Nagaraj B, Melngailis J, Ramesh R, Khriachtchev L, McDaniel E. 2002. Radiation damage and its recovery in focused ion beam fabricated ferroelectric capacitors. J Appl Phys 92:3275–3278.
Thompson LE, Rice PM, Delenia E, Lee VY, Brock PJ, Magbitang TP, Dubois G, Volksen W, Miller RD, Kim HC. 2006. Imaging thin films of nanoporous low-k dielectrics: Comparison between ultramicrotomy and focused ion beam preparations for transmission electron microscopy. Microsc Microanal 12:156–159.
Vetterli D, Dübeli M, Mühle R, Nebiker PW, Musil CR. 1995. Characterization of focused ion beam induced damage. Microelectron Eng 27:339–342.
Wang Z, Kato T, Hirayama T, Kato N, Sasaki K, Saka H. 2005. Surface damage induced by focused-ion-beam milling in a Si/Si p-n junction cross-sectional specimen. Appl Surf Sci 241:80–86.
Yabuuchi Y, Tametou S, Okano T, Inazato S, Sadayama S, Yamamoto Y, Iwasaki K, Sugiyama Y. 2004. A study of the damage on FIB-prepared TEM samples of AlxGa1-xAs. J Electron Microsc 53: 471–477.
Yonehara K, Baba N, Kanaya K. 1989. Application of ion-beam etching techniques to the fine structure of biological specimens as examined with a field emission SEM at low voltage. J Electron Microsc Tech 12:71–77.
Yu J, Liu J, Zhang J, Wu J. 2006. TEM investigation of FIB induced damages in preparation of metal material TEM specimens by FIB. Mater Lett 60:206–209.